Journal of Alloys and Compounds 495 (2010) 450–452

Contents lists available at ScienceDirect

Journal of Alloys and Compounds

journal homepage: www.elsevier.com/locate/jallcom

The fabrication and characteristic properties of amorphous $Co_{1-x}Zn_x$ alloy nanowire arrays

Y. Xu [a,*], J.L. Fu [b], D.Q. Gao [c], D.S. Xue [c]

[a] Physics Department, Xinxiang University, Xinxiang 453003, PR China
[b] College of Science, Minzu University of China, Beijing 100081, PR China
[c] Key Laboratory for Magnetism and Magnetic Materials of MOE, Lanzhou University, Lanzhou 730000, PR China

ARTICLE INFO

Article history:
Received 8 September 2008
Received in revised form 28 October 2009
Accepted 28 October 2009
Available online 5 November 2009

Keywords:
Amorphous materials
Nanostructures
X-ray diffraction

ABSTRACT

Amorphous Co–Zn alloy nanowire arrays with diameter of about 40 nm were fabricated in anodic aluminium oxide films by the electrodeposition method. Transmission electron microscope result shows that the nanowires are regular and uniform. Selected area electron diffraction and X-ray diffraction results indicate that the structure of nanowires is amorphous. Vibrating sample magnetometer is employed to study the magnetic properties of nanowire arrays at room temperature. The results show that the arrays of nanowires exhibit uniaxial magnetic anisotropy with the easy magnetization direction along the nanowire axes owing to the large shape anisotropy. When the applied magnetic field is parallel to the wire axis, the coercivity and squareness of the nanowire arrays decrease with increasing Zn concentration.

1. Introduction

In the past few years, great attention has been paid to the field of amorphous materials, due to their unique magnetic, chemical and electrical properties in basic research and new possible applications [1–3]. The ferromagnetic amorphous alloys can be used for electronic components, transformers and memory devices because they possess low coercivity, high magnetic permeability and other valuable technological properties [4–6].

The nanowire arrays have become the subject of intensive research due to their potential applications in ultra-high density magnetic storage devices and novel physical properties differing from those of their bulk counterparts [7–9]. Recently metal–metalloid Fe–P [10], Co–P [11], Ni–P [12] Co–Ni–P [13] and $Nd_5Fe_{95-x}B_x$ [14] amorphous nanowire arrays have been successfully explored. As far as amorphous nanowires are concerned, only a few examples of metal–metal alloy amorphous nanowires are reported in the literature. Li et al. fabricated the amorphous Co0.71Pt0.29 nanowire arrays by direct current electro-deposition [15]. For metal–metalloid systems, the dimension of metalloid atoms is so much discrepancy with metal atoms, so synthesizing metal–metalloid amorphous is easy. By contrast, synthesis and characteristics of metal–metal alloy amorphous nanowires is valuable.

The template synthesis in conjunction with electrochemical deposition has revealed itself to be an easy method of controlling compositions of amorphous nanowires [16–18]. Furthermore, it easily controls both length and the diameter of the pores [19–21]. In this paper, we report the fabrication of $Co_{1-x}Zn_x$ amorphous nanowire arrays by electrodeposition and investigate the structure and magnetic properties.

2. Experimental

The ordered anodic aluminum oxide (AAO) films were fabricated by a two-step anodizing process [16]. Briefly, the starting material, 99.9% pure Al foil, was degreased, annealed at 500 °C for about 2 h in open air. The foil was then dc anodized in 0.3 M oxalic acid aqueous solution under a constant voltage of 40 V at 0 °C for 4 h. An ordered porous alumina layer containing parallel pores with an average diameter of 40 nm was prepared. The electrodeposition of the Co–Zn alloy nanowire arrays was performed by using a standard double electrode bath. The AAO films are used as the anode, and the graphite is used as the cathode. The electrolyte contains $FeSO_4{\cdot}7H_2O$ (30 g/l), $ZnSO_4{\cdot}7H2O$ (5 g/l), H_3BO_4 (10 g/l), the AC electrodepositions were conducted at 200 Hz and 15 V for the duration of 5 min. The pH of each bath was adjusted to 3 with sulfuric acid. The compositions of $Co_{1-x}Zn_x$ nanowires were adjusted by varying the ratio of Co^{2+}: Zn^{2+} ions in the baths, Normally, the Co:Zn ratios in the starting electrolyte solution are different with the ratio in the final products [22]. The compositions in the $Co_{1-x}Zn_x$ nanowires were analyzed by an inductively coupled plasma-atomic emission spectrometer (IRIS, ER/S) with an uncertainty about +0.01.

The morphologies of the AAO films were obtained by using Field Emission Scanning Electron Microscope (FE-SEM Hitachi S-4800 ×). The nanowire arrays were separated from the AAO films by dissolving the aluminium oxide film in a solution of 1 M NaOH for transmission electron microscopy investigation. The images of Co–Zn nanowires were obtained by using a transmission electron microscopy (TEM, Hitachi H-600). Inductively coupled plasma-atomic emission spectrometer (IRIS, ER/S), selected area electron diffraction (SAED) and X-ray diffraction (XRD, X'Pert

* Corresponding author.
E-mail address: xuyan04@lzu.cn (Y. Xu).

0925-8388/$ – see front matter © 2009 Elsevier B.V. All rights reserved.
doi:10.1016/j.jallcom.2009.10.252

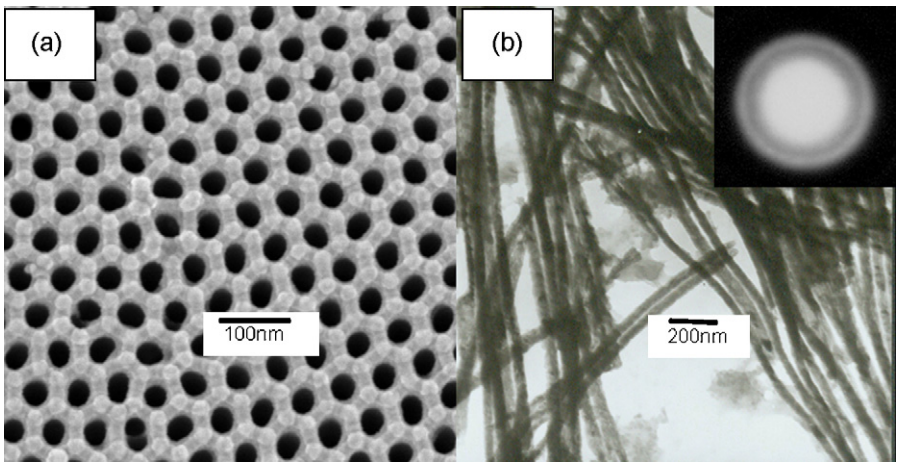

Fig. 1. (a) SEM image of AAO template and (b) TEM image and SAED pattern of the $Co_{0.74}Zn_{0.26}$ nanowires.

PRO PHILIPS, with Cu Kα radiation) were employed to study the chemical composition and structure of the nanowire arrays. The magnetic properties of nanowire arrays were characterized using a vibrating sample magnetometer (VSM, Lakeshore 7300) with the applied field parallel and perpendicular to the nanowire axis.

3. Result and discussion

3.1. The morphology of $Co_{0.74}Zn_{0.26}$ nanowires

An SEM image of the AAO films is shown in Fig. 1(a). It was found that the nanopores are uniform and ordered with diameters of about 40 nm. The SAED pattern and the TEM image of the $Co_{0.74}Zn_{0.26}$ nanowires with an aspect ratio about 70 are shown in Fig. 1(b). The TEM result shows that the average diameter of the nanowires is also about 40 nm, which is in agreement with the diameter of the nanopores embedded in the templates. The halo in the SAED pattern indicates that the nanowires are amorphous in structure.

Fig. 2 illustrates the XRD patterns of $Co_{1-x}Zn_x$ alloy nanowire arrays at different Zn composition. For $x < 0.18$, there are sharp peaks which can be indexed as (2 2 0), (4 0 0) and (4 4 0) of face-centered cubic of Co. With increasing Zn content in the nanowire arrays, the sharp peak gradually decreases. When the x reaches 0.26, the sharp diffraction peak disappears, which also reveals that the nanowire arrays are an amorphous structure, in agreement with the result of SAED. These results indicate that the $Co_{1-x}Zn_x$ alloy nanowire arrays gradually change from a crystalline phase to a homogenous amorphous phase with increasing the Zn content.

Fig. 3 shows the magnetic hysteresis curves of embedded $Co_{1-x}Zn_x$ nanowire array with $x = 0.26$, where //and (represent that the applied field H is parallel and perpendicular to the nanowire axis, respectively. The shapes of hysteresis loops is different in two directions, which indicate that the arrays exhibit anisotropy. It is known that the magnetocrystalline anisotropy is very weak in amorphous structure, so magnetic anisotropy of nanowires results from the shape anisotropy. In the amorphous nanowire arrays, as the interaction between wires is much weaker than that in the interior of wires, the shape anisotropy can be almost recognized as uniaxial magnetic anisotropy, and the easy magnetizing axis is parallel to the nanowires. In general, the coercivity H_c (//) is greater than H_c (() due to the anisotropy of the geometrical shape of the nanowires.

Fig. 4 shows the compositions of $Co_{1-x}Zn_x$ nanowires dependence of the coercivity and squareness of the magnetic hysteresis loops in parallel to the nanowire axis. With increasing Zn concentration x from 0 to 0.26, the coercivity H_c (//) decreases from 1900 to 1050 Oe and squareness Mr/Ms (//) decreases from 0.94 to 0.81. It is known that the remanence and coercivity depend on the magnetization reversal process. The chains-of-spheres model was used to interpret the magnetization reversal process in magnetic nanowires [22]. In the case of symmetric fanning, the parallel coercivity of the nanowires is proportional to the saturation magnetization Ms. With the Zn content increasing, the Ms of $Co_{1-x}Zn_x$ alloy nanowire arrays decrease, which is consistent with symmetric fanning model.

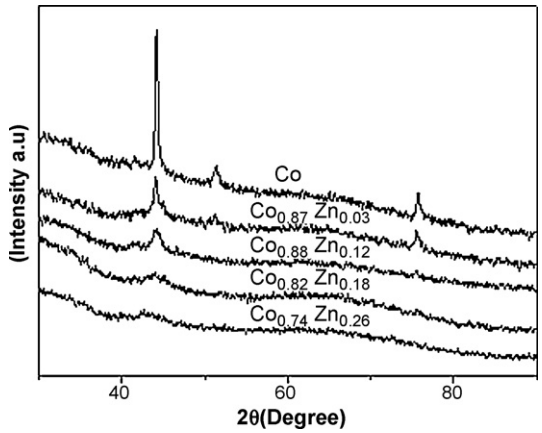

Fig. 2. X-ray diffraction patterns of AAO templates filled with $Co_{1-x}Zn_x$ nanowires of various compositions.

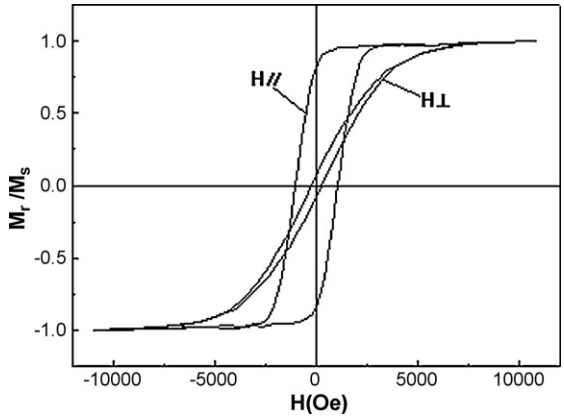

Fig. 3. RT magnetic hysteresis loops of $Co_{0.74}Zn_{0.26}$ nanowires embedded in AAO templates.

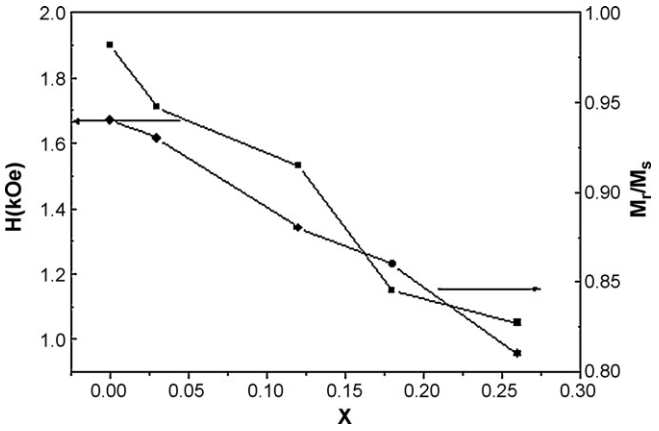

Fig. 4. Composition dependence of coercivity and squareness in parallel to the nanowires of $Co_{1-x}Zn_x$ nanowires.

4. Conclusions

In conclusion, the arrays of $Co_{1-x}Zn_x$ amorphous nanowires with diameters about 40 nm were fabricated in AAO templates by the electrodeposition method. The structure and magnetic properties of the arrays were investigated. With the Zn content increasing, the $Co_{1-x}Zn_x$ alloy nanowire arrays gradually change from a crystalline phase to a homogenous amorphous phase, and the coercivity in parallel to the nanowire axis decreases. Due to the shape anisotropy effect, the arrays of nanowires exhibit obviously uniaxial magnetic anisotropy and the easy magnetizing axis is parallel to the nanowires.

Acknowledgment

This work is supported by NSFC (grant no. 50671046).

References

[1] M. Maurer, M.C. Cadeville, J.P. Sanchez, J. Phys. F: Met. Phys. 9 (1979) 271.
[2] T. Kazuhide, Y. Matsumi, S. Kenji, J. Phys. Soc. Jpn. 51 (1982) 3882.
[3] C.C. Koch, O.B. Cavin, C.G. McKamey, J.O. Scarbrough, Appl. Phys. Lett. 43 (1983) 1017.
[4] E.P. Elsukov, Yu N. Vorobev, A.V. Trubachev, V.A. Barinov, Phys. Status Solidi a 117 (1990) 291.
[5] S. Armyanov, S. Vitkova, O. Blaoiev, J. Appl. Electrochem. 27 (1997) 185.
[6] R.C. Silva, L. Sartorelli, M.M. Sardela, A.A. Pasa, Phys. Status Solidi a 187 (2001) 85.
[7] T.M. Whitney, J.S. Jiang, P.C. Searson, C.L. Chien, Science 261 (1993) 1316.
[8] N. Zabala, M.J. Puska, R.M. Nieminen, Phys. Rev. Lett. 80 (1998) 3336.
[9] J. Jorritsma, J.A. Mydosh, J. Appl. Phys. 84 (1998) 901.
[10] D.S. Xue, H.G. Shi, Nanotechnology 15 (2004) 1752.
[11] X.Y. Yuan, G.S. Wu, T. Xie, Y. Lin, L.D. Zhang, Nanotechnology 15 (2004) 59.
[12] H. Chiriac, A.E. Moga, M. Urse, I. Paduraru, N. Lupu, J. Magn. Magn. Mater. 272 (2004) 1678.
[13] X.Y. Yuan, G.S. Wu, T. Xie, Y. Lin, G.W. Meng, L.D. Zhang, Solid State Commun. 130 (2004) 429.
[14] D.Q. Gao, J.L. Fu, Y. Xu, D.S. Xue, Mater. Lett. 62 (2008) 3070.
[15] H. Li, C.L. Xu, G.Y. Zhao, Y.K. Su, T. Xu, H.L. Li, Solid State Commun. 132 (2004) 399.
[16] H. Masuda, K. Fukuda, Science 268 (1995) 1466.
[17] C.Y. Yu, Y.L. Yu, H.Y. Sun, T. Xu, X.H. Li, W. Li, et al., Mater. Lett. 61 (2007) 1859.
[18] X.W. Wang, G.T. Fei, K. Zheng, Z. Jin, L.D. Zhang, Appl. Phys. Lett. 88 (2006) 1–3.
[19] P.S. Fodor, G.M. Tsoi, L.E. Wenger, J. Appl. Phys. 91 (2002) 8186.
[20] S.K. Hwang, J. Lee, S.H. Jeong, P.S. Lee, K.H. Lee, Nanotechnology 16 (2005) 850.
[21] J.B. Wang, X.Z. Zhou, Q.F. Liu, D.S. Xue, F.S. Li, B. Li, Nanotechnology 15 (2004) 485.
[22] Q.F. Zhan, Z.Y. Chen, D.S. Xue, F.S. Li, Phys. Rev. B 66 (2002) 1344366.